



Inhibition of *Helicobacter pylori* aminoacyl-tRNA amidotransferase by chloramphenicol analogs

Christian Balg^a, Maria De Mieri^c, Jonathan L. Huot^b, Sébastien P. Blais^b, Jacques Lapointe^b, Robert Chênevert^{a,*}

^aDépartement de Chimie, PROTEO, Faculté des Sciences et de Génie, Université Laval, Québec, Canada G1V 0A6

^bDépartement de Biochimie et de Microbiologie, PROTEO, Faculté des Sciences et de Génie, Université Laval, Québec, Canada G1V 0A6

^cDipartimento di Chimica, Biochimica e Biotecnologie per la Medicina, Università degli Studi di Milano, 20133 Milano, Italy

ARTICLE INFO

Article history:

Received 5 July 2010

Revised 14 September 2010

Accepted 18 September 2010

Available online 1 October 2010

Keywords:

Chloramphenicol

Amidotransferase

Aminoacyl-tRNA

Transamidation

GatCAB

Helicobacter pylori

Puromycin

ABSTRACT

Genomic studies revealed the absence of glutamyl-tRNA synthetase and/or asparaginyl-tRNA synthetase in many bacteria and all known archaea. In these microorganisms, glutamyl-tRNA^{Gln} (Gln-tRNA^{Gln}) and/or asparaginyl-tRNA^{Asn} (Asn-tRNA^{Asn}) are synthesized via an indirect pathway involving side chain amidation of misacylated glutamyl-tRNA^{Gln} (Glu-tRNA^{Gln}) and/or aspartyl-tRNA^{Asn} (Asp-tRNA^{Asn}) by an amidotransferase. A series of chloramphenicol analogs have been synthesized and evaluated as inhibitors of *Helicobacter pylori* GatCAB amidotransferase. Compound **7a** was identified as the most active competitive inhibitor of the transamidase activity with respect to Asp-tRNA^{Asn} ($K_m = 2 \mu\text{M}$), with a K_i value of $27 \mu\text{M}$.

© 2010 Elsevier Ltd. All rights reserved.

1. Introduction

The specific aminoacylation of tRNAs is essential for the faithful translation of the genetic information into proteins. Aminoacyl-tRNA synthetases (aaRS) are the enzymes that catalyze the esterification reaction between an amino acid and its cognate tRNA.^{1,2} In the cytoplasm of eukaryotic cells, the pairing of glutamine and asparagine with their corresponding tRNA proceeds through a direct pathway involving a glutamyl-tRNA synthetase (GlnRS) and an asparaginyl-tRNA synthetase (AsnRS), respectively (Fig. 1A). Genomic studies revealed the absence of GlnRS and/or AsnRS in all known archaea, in many bacteria, and in some organelles. The alternative indirect pathway for the formation of Gln-tRNA^{Gln} and Asn-tRNA^{Asn} involves the misacylation of tRNA^{Gln} with Glu (or tRNA^{Asn} with Asp) by a nondiscriminating aminoacyl-tRNA synthetase (ND-aaRS) followed by the transamidation of the misacylated aa-tRNA by an amidotransferase (AdT) (Fig. 1B).^{3,4}

Two types of AdT are found in nature, a heterotrimeric (GatCAB) and a heterodimeric protein (GatDE). GatCAB uses both Glu-tRNA^{Gln} and Asp-tRNA^{Asn} as substrates and is present in bacteria, archaea and some organelles, while GatDE functions solely

as a Glu-tRNA^{Gln} amidotransferase and is found only in archaea.⁵ Crystal structures of GatCAB and GatDE have been determined recently.^{6–9}

The transamidation of the misacylated Glu-tRNA^{Gln} and/or Asp-tRNA^{Asn} by the GatCAB-type aminoacyl-tRNA amidotransferase (AdT) involves three distinct events (Fig. 2). Glutamine is hydrolyzed in the GatA subunit serine-based glutaminase site to generate ammonia, which reaches GatB through a molecular tunnel. In the GatB subunit, the side-chain carboxyl group of the misacylated-tRNA is activated by ATP to form a phosphoryl-Glu-tRNA^{Gln} or a phosphoryl-Asp-tRNA^{Asn} intermediate (kinase step). In the final transamidase step, the enzyme-bound ammonia reacts with the high-energy mixed anhydride to yield the corresponding amide side-chain (Gln-tRNA^{Gln} or Asn-tRNA^{Asn}). The small GatC subunit

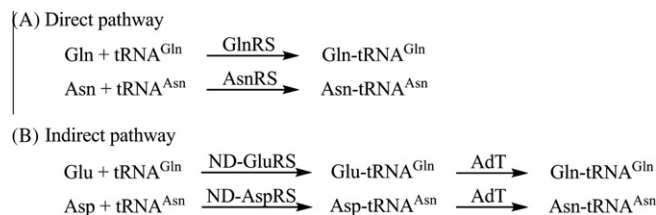


Figure 1. Glutamyl-tRNA and asparaginyl-tRNA biosynthetic pathways. ND-aaRS = nondiscriminating aminoacyl-tRNA synthetase; AdT = amidotransferase.

* Corresponding author. Tel.: +1 418 656 3283; fax: +1 418 656 7916.

E-mail address: robert.chenevert@chm.ulaval.ca (R. Chênevert).

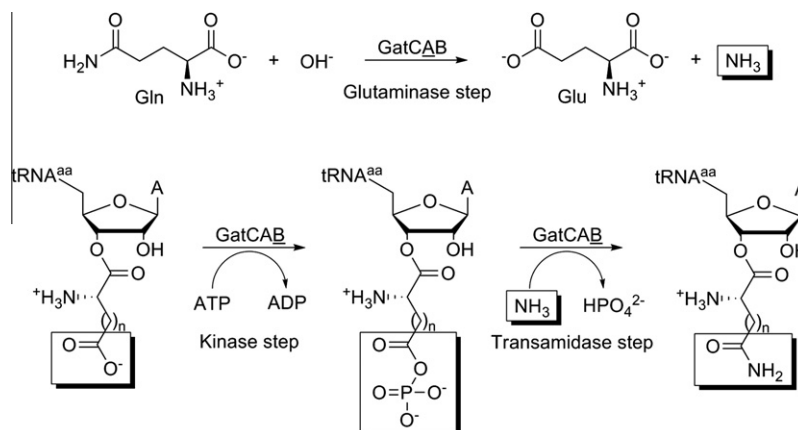


Figure 2. Reaction mechanism of GatCAB aminoacyl-tRNA amidotransferase. A = Adenine; aa = Asn, $n = 1$; aa = Gln, $n = 2$. For each of the three reactions represented here, the catalysis takes place in the subunit whose symbol (A or B) is underlined in GatCAB.

wraps around the interface of the A- and B-subunits, suggesting that it may stabilize the complex.

For bacteria lacking a GlnRS or AsnRS, AdT activity is essential for protein biosynthesis.¹⁰ Therefore, inhibition of this enzyme could provide a novel basis for the development of selective antimicrobial agents.¹¹ Only a few AdT inhibitors have been reported so far. Some analogs of ATP were useful to study the reaction mechanism.¹² Glutamyl- γ -boronate derivatives were evaluated as serine inactivators in the AdT-glutaminase active site; these inhibitors provided potent inhibition in vitro and displayed antibacterial activities for many AdT-dependent bacteria.¹³ Recently, we reported the inhibition of *Helicobacter pylori* GatCAB aminoacyl-tRNA amidotransferase by puromycin (**1**, Fig. 3) analogs.^{14,15} Compound **2** was found to have the most potent inhibitory activity against GatCAB ($K_i = 4 \mu\text{M}$ with respect to Asp-tRNA^{Asn}). Our strategy was based on the premise that the sulfone moiety mimics the transition state in the transamidation reaction (last step in Fig. 2).

The antibiotic chloramphenicol **3** inhibits protein synthesis by binding to the peptidyl transferase region of the ribosome, and overlaps the binding site of puromycin.¹⁶ In the search of novel AdT inhibitors, this similarity and the structural relationship of the two compounds led us to explore the potential of L-methionine-sulfone derivatives of chloramphenicol as inhibitors of GatCAB aminoacyl-tRNA amidotransferase.

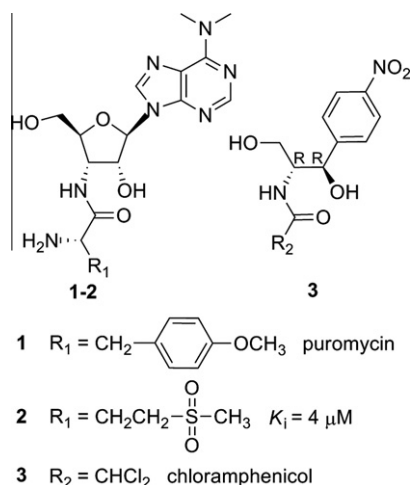


Figure 3. Chemical structures of puromycin **1**, AdT inhibitor **2** and chloramphenicol **3**.

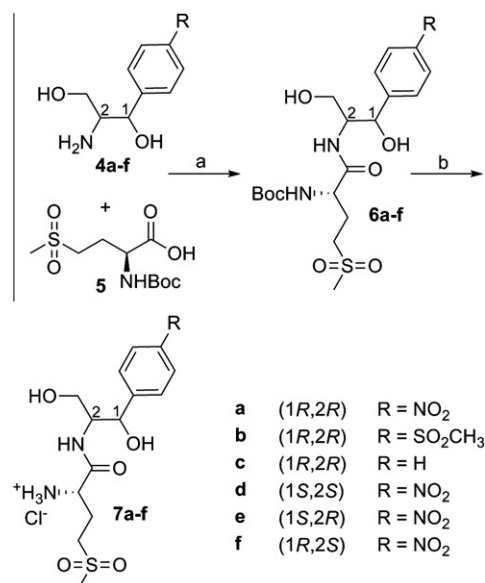
2. Results and discussion

2.1. Synthesis of chloramphenicol derivatives (7a–f)

The synthesis of chloramphenicol analogs **7a–f** is outlined in Scheme 1. Amines **4a–f** were condensed with commercially available *N*-Boc-methionine-sulfone **5** under standard conditions using 1-(3-dimethylaminopropyl)-3-ethylcarbodiimide hydrochloride (EDC)/*N*-hydroxysuccinimide in DMF. Amino-alcohol **4a–d** are commercially available whereas **4e** and **4f** were prepared from **4a** and **4d**, respectively using a literature procedure.¹⁷ Treatment of **6a–f** with 4 M HCl/dioxane resulted in cleavage of the *N*-tert-butoxycarbonyl group to provide the corresponding amides **7a–f**. These compounds were isolated after precipitation in Et₂O as the hydrochloride salts.

2.2. Inhibition of *H. pylori* GatCAB amidotransferase (AdT)

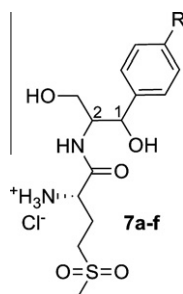
Chloramphenicol **3** and analogs **7a–f** were evaluated for in vitro inhibitory activity against *H. pylori* GatCAB aminoacyl-tRNA amidotransferase (Table 1). Enzyme production and kinetic



Scheme 1. Reagents and conditions: (a) EDC, *N*-hydroxysuccinimide, DMF, 24 h (b) 4 M HCl/dioxane, 40 min.

Table 1

Inhibition of *H. pylori* GatCAB aminoacyl-tRNA amidotransferase (AdT) by chloramphenicol and several analogs



Compound	R	Stereochemistry	K_i (μM) \pm standard error
Chloramphenicol 3	NO ₂	(1 <i>R</i> ,2 <i>R</i>)	1850 \pm 550
7a	NO ₂	(1 <i>R</i> ,2 <i>R</i>)	27 \pm 6
7b	SO ₂ CH ₃	(1 <i>R</i> ,2 <i>R</i>)	120 \pm 24
7c	H	(1 <i>R</i> ,2 <i>R</i>)	400 \pm 100
7d	NO ₂	(1 <i>S</i> ,2 <i>S</i>)	160 \pm 20
7e	NO ₂	(1 <i>S</i> ,2 <i>R</i>)	2800 \pm 500
7f	NO ₂	(1 <i>R</i> ,2 <i>S</i>)	370 \pm 40

Standard errors were calculated by curve-fitting of our data, using KALEIDAGRAPH 4.0 (Synergy Software). Values calculated from averages of two distinct experiments (four, for **7a**), weighting by inverse variance.¹⁸

experiments were carried out as previously described.¹⁴ Competitive inhibition with respect to Asp-tRNA^{Asn} was observed for all compounds.

The parent compound chloramphenicol **3** is a very weak inhibitor of GatCAB ($K_i \approx 1.9$ mM). Replacement of the dichloroacetyl moiety of chloramphenicol by L-methionyl-sulfone considerably enhances the activity and **7a** was identified as the most active inhibitor with a K_i value of 27 μM . Replacement of the *para*-nitro group by a sulfone (**7b**, related to thiamphenicol) or a hydrogen (**7c**) decreased the ability to inhibit GatCAB ($K_i = 120$ and 400 μM , respectively). In order to complete this structure–activity relationship study, we evaluated the effect of the configurations at C-1 and C-2 stereogenic centers on the activity. The (1*S*,2*S*) enantiomer **7d** exhibited a moderate five-fold decrease in activity ($K_i = 160$ μM for **7d** versus 27 μM for **7a**). Diastereoisomers (1*S*,2*R*)-**7e** and (1*R*,2*S*)-**7f** were less active derivatives ($K_i = 2.8$ mM and 370 μM , respectively) and, in particular, the loss in potency was more marked for (1*S*,2*R*) analog than for the (1*R*,2*S*) isomer.

The structural similarity of puromycin, chloramphenicol and the aminoacyl-adenosyl terminus of tRNA has already been stressed. Aminoacyl analogs of chloramphenicol were evaluated as inhibitors of the peptide bond formation in a ribosomal cell-free system derived from *Escherichia coli*.^{19–21} There is however a major difference between the ribosomal peptidyl transferase and the amidotransferase reactions. In the peptidyl transfer, the ester (α -position) of the P-site peptidyl-tRNA is attacked by the α -amino group of the A-site aminoacyl-tRNA. In contrast, the aminoacyl-tRNA amidotransferase reaction is the simple conversion of the side chain carboxylic acid (β -position for Asp, γ -position for Glu) into an amide (Asn or Gln) while the amino acid is still attached to a tRNA (pre-translational modification). The enzyme is equally efficient in transamidation of both Asp-tRNA^{Asn} and Glu-tRNA^{Gln}.³ Although the detailed interactions of inhibitors **7a–f** with GatCAB are yet to be defined, the sulfone moiety of **7a** can be considered as a stable analog of the transition state in the last step of the transamidation process, where the carbonyl to be attacked by ammonia is replaced by a tetrahedral sulfur atom with a methyl group mimicking ammonia (Fig. 4). Various sulfur or phosphorus-containing derivatives have been proposed as analogs of the tetrahedral intermediate formed during enzymatic reactions involving hydrolysis or formation of

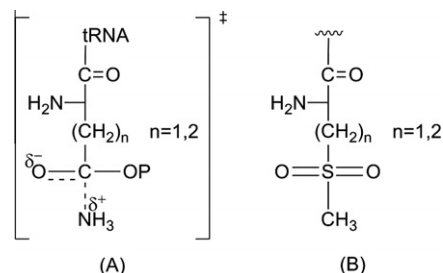


Figure 4. Analogy between a putative transition state of the transamidase step (A) and the sulfone side chain of inhibitors **7a–f** (B).

amide functionalities.²² The *p*-nitro group and the (1*R*,2*R*) stereochemistry of chloramphenicol combined with the L-methionyl-sulfone moiety appeared to be optimal in this series. Given the much smaller number of possible contacts between **7a** and GatCAB when compared to those possible for Asp-tRNA^{Asn}, it is noteworthy that the K_i for **7a** is only ten times greater than the K_m for the natural substrate.

Chloramphenicol analogs **7a–f** represent a new class of AdT inhibitors and may provide the basis for the design of other low-molecular weight inhibitors. Further investigation is currently underway to find more potent inhibitors of GatCAB amidotransferase based on compound **7a**.

3. Experimental

3.1. General

Chemical reagents were purchased from Aldrich–Sigma Chemical Company. Flash column chromatography was carried out using 40–63 μM (230–400 mesh) silica gel. Optical rotations were measured using a JASCO DIP-360 digital polarimeter (c as g of compound per 100 mL). Infrared spectra were recorded on a Bomem MB-100 spectrometer. NMR spectra were recorded on a Varian Inova AS400 spectrometer (400 MHz). Mass spectra were obtained on an Agilent 6210 ESI TOFMS.

3.2. Typical procedure for preparation of amides **6a–f**

Amine **4a** (25.0 mg, 118 μmol), *N*-Boc-L-methionine-sulfone **5** (36.5 mg, 130 μmol), *N*-hydroxysuccinimide (14.9 mg, 130 μmol) and EDC (27.1 mg, 141 μmol) were dissolved in anhydrous DMF (1.0 mL). The mixture was stirred at room temperature for 24 h. The solvent was coevaporated with toluene and the residue was purified by flash chromatography (7–8% MeOH/CH₂Cl₂) to yield **6a** (42.3 mg, 76%).

3.2.1. (1*R*,2*R*)-1-(4-Nitrophenyl)-2-(*N*^α-Boc-L-methionyl-sulfone-amido)-1,3-propadiol (**6a**)

White solid; mp 77–79 °C; $[\alpha]_D^{21} -43.5$ (c 0.84, CH₂Cl₂); IR (KBr) 3400, 2979, 1666, 1521, 1349, 1294, 1164, 1129 cm⁻¹; ¹H NMR (400 MHz, CD₃OD) δ 1.42 (s, 9H), 1.85–1.97 (m, 1H), 1.97–2.07 (m, 1H), 2.89 (s, 3H), 3.01 (t, *J* = 8.1 Hz, 2H), 3.55 (dd, *J* = 10.8 and 6.5 Hz, 1H), 3.74 (dd, *J* = 10.8 and 6.9 Hz, 1H), 4.06–4.15 (m, 2H), 5.07 (d, *J* = 2.0 Hz, 1H), 7.60 (d, *J* = 8.5 Hz, 2H), 8.14 (d, *J* = 8.8 Hz, 2H); ¹³C NMR (100 MHz, CD₃OD) δ 25.0, 27.5, 39.3, 50.6, 53.2, 56.5, 61.4, 70.4, 79.8, 123.0, 127.2, 147.3, 150.6, 156.4, 172.3; HRMS (ESI) calcd for C₁₉H₂₉N₃O₅Sn [M+Na]⁺ 498.1517. Found: 498.1514.

3.2.2. (1*R*,2*R*)-1-(4-Methylsulfonylphenyl)-2-(*N*^α-Boc-L-methionyl-sulfone-amido)-1,3-propadiol (**6b**)

White solid; yield 52%; mp 90–92 °C; $[\alpha]_D^{21} -32.6$ (c 0.60, MeOH); IR (KBr) 3370, 2931, 1668, 1523, 1299, 1149 cm⁻¹; ¹H

NMR (400 MHz, CD₃OD) δ 1.44 (s, 9H), 1.85–1.96 (m, 1H), 1.96–2.07 (m, 1H), 2.90 (s, 3H), 2.98–3.06 (m, 2H), 3.07 (s, 3H), 3.53 (dd, J = 10.7 and 6.4 Hz, 1H), 3.72 (dd, J = 10.8 and 7.0 Hz, 1H), 4.05–4.13 (m, 2H), 5.04–5.08 (m, 1H), 7.63 (d, J = 8.2 Hz, 2H), 7.86 (d, J = 8.4 Hz, 2H); ¹³C NMR (100 MHz, CD₃OD) δ 24.9, 27.5, 39.4, 43.4, 50.7, 53.5, 56.5, 61.3, 70.4, 79.9, 127.0, 127.2, 139.6, 149.4, 156.5, 172.3; HRMS (ESI) calcd for C₂₀H₃₂N₂O₉S₂Na [M+Na]⁺ 531.1441. Found: 531.1448.

3.2.3. (1R,2R)-1-Phenyl-2-(N^α-Boc-L-methionyl-sulfone-amido)-1,3-propadiol (6c)

White solid; yield 81%; mp 55–57 °C; $[\alpha]_D^{21}$ –41.1 (c 0.38, MeOH); IR (KBr) 3387, 2979, 1694, 1664, 1521, 1292, 1165, 1128, 1053 cm^{–1}; ¹H NMR (400 MHz, CD₃OD) δ 1.44 (s, 9H), 1.89–2.02 (m, 1H), 2.02–2.14 (m, 1H), 2.89 (s, 3H), 2.96–3.10 (m, 2H), 3.44 (dd, J = 10.0 and 6.4 Hz, 1H), 3.63 (dd, J = 10.2 and 6.2 Hz, 1H), 4.01–4.09 (m, 1H), 4.09–4.18 (m, 1H), 7.20 (t, J = 7.1 Hz, 1H), 7.29 (t, J = 7.4 Hz, 2H), 7.36 (d, J = 7.4 Hz, 2H); ¹³C NMR (100 MHz, CD₃OD) δ 25.0, 27.5, 39.3, 50.6, 53.5, 57.1, 61.2, 71.4, 79.9, 126.2, 127.3, 128.1, 142.4, 156.5, 172.3; HRMS (ESI) calcd for C₁₉H₃₀N₂O₇SNa [M+Na]⁺ 453.1666. Found: 453.1669.

3.2.4. (1S,2S)-1-(4-Nitrophenyl)-2-(N^α-Boc-L-methionyl-sulfone-amido)-1,3-propadiol (6d)

White solid; yield 87%; mp 82–85 °C; $[\alpha]_D^{21}$ –0.58 (c 0.90, MeOH); IR (KBr) 3409, 2979, 1665, 1521, 1350, 1294, 1164, 1128 cm^{–1}; ¹H NMR (400 MHz, CD₃OD) δ 1.42 (s, 9H), 1.70–1.83 (m, 1H), 1.93–2.05 (m, 1H), 2.78–2.97 (m, 5H), 3.57 (dd, J = 10.9 and 5.9 Hz, 1H), 3.74 (dd, J = 10.8 and 7.3 Hz, 1H), 4.08 (dd, J = 8.5 and 5.2 Hz, 1H), 4.11–4.17 (m, 1H), 5.10 (d, J = 1.7 Hz, 1H), 7.61 (d, J = 8.6 Hz, 2H), 8.16 (d, J = 8.8 Hz, 2H); ¹³C NMR (100 MHz, CD₃OD) δ 25.3, 27.5, 39.3, 50.6, 53.0, 56.6, 61.4, 70.1, 79.8, 123.1, 127.1, 147.4, 150.8, 156.4, 172.2; HRMS (ESI) calcd for C₁₉H₂₉N₃O₉SNa [M+Na]⁺ 498.1517. Found: 498.1511.

3.2.5. (1S,2R)-1-(4-Nitrophenyl)-2-(N^α-Boc-L-methionyl-sulfone-amido)-1,3-propadiol (6e)

White solid; yield 84%; mp 171–173 °C (dec); $[\alpha]_D^{21}$ –18.4 (c 0.96, CH₂Cl₂/MeOH 1:1); IR (KBr) 3426, 3342, 2982, 1681, 1658, 1522, 1348, 1285, 1163, 1129, 1051 cm^{–1}; ¹H NMR (400 MHz, CD₃OD) δ 1.39 (s, 9H), 1.83–1.95 (m, 1H), 1.95–2.08 (m, 1H), 2.89 (s, 3H), 3.03 (t, J = 7.8 Hz, 2H), 3.64 (dd, J = 10.9 and 2.8 Hz, 1H), 3.78 (dd, J = 10.8 and 6.4 Hz, 1H), 4.00–4.14 (m, 2H), 4.80 (d, J = 7.5 Hz, 1H), 7.60 (d, J = 8.2 Hz, 2H), 8.24 (d, J = 8.2 Hz, 2H); ¹³C NMR (100 MHz, CD₃OD) δ 25.1, 27.4, 39.3, 50.6, 53.3, 56.6, 60.3, 72.3, 79.8, 123.0, 127.8, 147.5, 150.0, 156.4, 172.0; HRMS (ESI) calcd for C₁₉H₂₉N₃O₉SNa [M+Na]⁺ 498.1517. Found: 498.1530.

3.2.6. (1R,2S)-1-(4-Nitrophenyl)-2-(N^α-Boc-L-methionyl-sulfone-amido)-1,3-propadiol (6f)

White solid; yield 72%; mp 175–176 °C (dec); $[\alpha]_D^{21}$ –10.8 (c 1.70, MeOH); IR (KBr) 3424, 3357, 2978, 1681, 1660, 1523, 1350, 1294, 1166, 1131, 1053 cm^{–1}; ¹H NMR (400 MHz, CD₃OD) δ 1.43 (s, 9H), 1.64–1.74 (m, 1H), 1.80–1.88 (m, 1H), 2.87 (s, 3H), 2.83–2.89 (m, 2H), 3.70 (dd, J = 11.2 and 3.7 Hz, 1H), 3.86 (dd, J = 11.3 and 5.5 Hz, 1H), 4.03 (dd, J = 8.5 and 5.1 Hz, 1H), 4.15–4.19 (m, 1H), 4.82 (d, J = 8.1 Hz, 1H), 7.63 (d, J = 8.6 Hz, 2H), 8.20 (d, J = 8.8 Hz, 2H); ¹³C NMR (100 MHz, CD₃OD) δ 26.5, 28.7, 40.6, 51.8, 54.4, 57.6, 61.9, 73.4, 81.1, 124.6, 129.3, 149.0, 151.4, 157.7, 173.1; HRMS (ESI) calcd for C₁₉H₂₉N₃O₉SNa [M+Na]⁺ 498.1517. Found: 498.1505.

3.3. Typical procedure for the cleavage of the N-tert-butoxycarbonyl groups

A solution of compound **6a** (41.9 mg, 88.1 μmol) in 4 M HCl/dioxane (2.0 mL) was stirred at room temperature for 40 min.

The solvent was coevaporated under reduced pressure with MeOH. The residue was dissolved in a minimum of EtOH (2.0 mL) and the product was precipitated by the addition of Et₂O (20 mL). The product was collected by filtration and washed with Et₂O to give **7a** (30.3 mg, 84%).

3.3.1. (1R,2R)-1-(4-Nitrophenyl)-2-(L-methionyl-sulfone-amido)-1,3-propadiol (7a)

White solid; mp 140–143 °C (dec); $[\alpha]_D^{21}$ 14.6 (c 0.19, MeOH/H₂O 1:1); IR (KBr) 3386, 2926, 1683, 1520, 1351, 1286, 1133 cm^{–1}; ¹H NMR (400 MHz, CD₃OD) δ 2.21–2.39 (m, 2H), 2.99 (s, 3H), 3.27 (t, J = 8.0 Hz, 2H), 3.54 (dd, J = 10.9 and 7.4 Hz, 1H), 3.77 (dd, J = 10.9 and 5.4 Hz, 1H), 4.03 (t, J = 6.3 Hz, 1H), 4.17–4.25 (m, 1H), 5.02 (d, J = 3.7 Hz, 1H), 7.65 (d, J = 8.9 Hz, 2H), 8.17 (d, J = 8.8 Hz, 2H); ¹³C NMR (100 MHz, CD₃OD) δ 24.4, 39.6, 49.1, 51.5, 57.4, 61.6, 70.7, 123.1, 127.3, 147.5, 150.4, 167.8; HRMS (ESI) calcd for C₁₄H₂₂N₃O₇S [M+H]⁺ 376.1173. Found: 376.1184.

3.3.2. (1R,2R)-1-(4-Methylsulfonylphenyl)-2-(L-methionyl-sulfone-amido)-1,3-propadiol (7b)

White solid; yield quant.; mp 135–137 °C (dec); $[\alpha]_D^{21}$ 8.3 (c 0.39, MeOH); IR (KBr) 3434, 2924, 1679, 1286, 1147 cm^{–1}; ¹H NMR (400 MHz, CD₃OD) δ 2.21–2.40 (m, 2H), 2.99 (s, 3H), 3.09 (s, 3H), 3.28 (t, J = 7.9 Hz, 2H), 3.52 (dd, J = 10.9 and 7.3 Hz, 1H), 3.75 (dd, J = 11.0 and 5.4 Hz, 1H), 4.05 (t, J = 6.3 Hz, 1H), 4.17–4.23 (m, 1H), 5.00 (d, J = 3.8 Hz, 1H), 7.67 (d, J = 8.3 Hz, 2H), 7.89 (d, J = 8.3 Hz, 2H); ¹³C NMR (100 MHz, CD₃OD) δ 24.4, 39.6, 43.2, 49.1, 51.5, 57.5, 61.5, 70.8, 127.2, 127.3, 139.8, 149.2, 167.8; HRMS (ESI) calcd for C₁₅H₂₅N₂O₇S₂ [M+H]⁺ 409.1098. Found: 409.1099.

3.3.3. (1R,2R)-1-Phenyl-2-(L-methionyl-sulfone-amido)-1,3-propadiol (7c)

White solid; yield quant.; mp 120–125 °C (dec); $[\alpha]_D^{21}$ 0.65 (c 0.48, MeOH); IR (KBr) 3425, 2923, 1684, 1561, 1496, 1285, 1133, 1056 cm^{–1}; ¹H NMR (400 MHz, CD₃OD) δ 2.24–2.43 (m, 2H), 2.99 (s, 3H), 3.25–3.35 (m, 2H), 3.41 (dd, J = 10.9 and 7.2 Hz, 1H), 3.61 (dd, J = 11.0 and 4.6 Hz, 1H), 4.07 (t, J = 6.1 Hz, 1H), 4.12–4.19 (m, 1H), 4.81 (d, J = 5.9 Hz, 1H), 7.24 (t, J = 7.3 Hz, 1H), 7.31 (t, J = 7.4 Hz, 2H), 7.39 (d, J = 7.3 Hz, 2H); ¹³C NMR (100 MHz, CD₃OD) δ 24.3, 39.7, 49.2, 51.7, 57.9, 61.2, 72.1, 126.4, 127.6, 128.2, 142.2, 167.9; HRMS (ESI) calcd for C₁₄H₂₃N₂O₅S [M+H]⁺ 331.1322. Found: 331.1319.

3.3.4. (1S,2S)-1-(4-Nitrophenyl)-2-(L-methionyl-sulfone-amido)-1,3-propadiol (7d)

White solid; yield 91%; mp 85–90 °C (dec); $[\alpha]_D^{21}$ 19.4 (c 0.53, MeOH); IR (KBr) 3426, 2925, 1679, 1519, 1351, 1285, 1134 cm^{–1}; ¹H NMR (400 MHz, CD₃OD) δ 1.95–2.14 (m, 2H), 2.71–2.82 (m, 1H), 2.84–2.94 (m, 4H), 3.60 (dd, J = 10.9 and 6.3 Hz, 1H), 3.78 (dd, J = 10.9 and 6.5 Hz, 1H), 4.00 (t, J = 6.3 Hz, 1H), 4.23–4.30 (m, 1H), 5.09 (d, J = 3.2 Hz, 1H), 7.66 (d, J = 8.6 Hz, 2H), 8.19 (d, J = 8.8 Hz, 2H); ¹³C NMR (100 MHz, CD₃OD) δ 24.3, 39.6, 49.2, 51.6, 57.0, 61.5, 70.2, 123.3, 127.1, 147.5, 150.8, 167.7; HRMS (ESI) calcd for C₁₄H₂₂N₃O₇S [M+H]⁺ 376.1173. Found: 376.1167.

3.3.5. (1S,2R)-1-(4-Nitrophenyl)-2-(L-methionyl-sulfone-amido)-1,3-propadiol (7e)

White solid; yield 81%; mp 185–190 °C (dec); $[\alpha]_D^{21}$ 18.0 (c 0.58, MeOH); IR (KBr) 3351, 2927, 1683, 1519, 1351, 1285, 1133 cm^{–1}; ¹H NMR (400 MHz, CD₃OD) δ 2.20–2.40 (m, 2H), 2.98 (s, 3H), 3.27 (t, J = 8.0 Hz, 2H), 3.63–3.74 (m, 2H), 3.99 (t, J = 6.4 Hz, 1H), 4.15–4.22 (m, 1H), 4.88 (dd, J = 6.4 Hz, 1H), 7.64 (d, J = 8.4 Hz, 2H), 8.20 (d, J = 8.8 Hz, 2H); ¹³C NMR (100 MHz, CD₃OD) δ 24.6, 39.6, 49.1, 51.6, 57.3, 59.8, 72.4, 123.2, 127.5, 147.6, 149.9, 167.6; HRMS (ESI) calcd for C₁₄H₂₂N₃O₇S [M+H]⁺ 376.1173. Found: 376.1186.

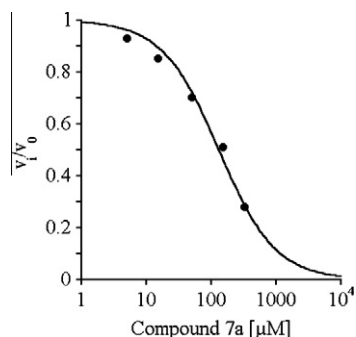


Figure 5. Compound **7a** is a competitive inhibitor of *H. pylori* AdT with respect to *H. pylori* Asp-tRNA^{Asn}. A K_i of $27 \pm 6 \mu\text{M}$ was obtained by fitting the data points to the competitive inhibition equation described above for four experiments, and the calculated values were weighted by inverse variance.

3.3.6. (1R,2S)-1-(4-Nitrophenyl)-2-(L-methionyl-sulfone-amido)-1,3-propadiol (**7f**)

White solid; yield 75%; mp 165–170 °C (dec); $[\alpha]_D^{21} -1.8$ (c 1.00, MeOH); IR (KBr) 3409, 2925, 1683, 1520, 1352, 1286, 1135 cm^{-1} ; ^1H NMR (400 MHz, CD_3OD) δ 1.88–2.09 (m, 2H), 2.70–2.90 (m, 2H), 2.92 (s, 3H), 3.72–3.86 (m, 2H), 3.90–3.99 (m, 1H), 4.23–4.33 (m, 1H), 4.84 (d, $J = 8.0$ Hz, 1H), 7.66 (d, $J = 8.5$ Hz, 2H), 8.22 (d, $J = 8.5$ Hz, 2H); ^{13}C NMR (100 MHz, CD_3OD) δ 25.2, 40.7, 50.2, 52.8, 57.5, 61.7, 73.1, 124.5, 129.2, 148.9, 150.9, 168.4; HRMS (ESI) calcd for $\text{C}_{14}\text{H}_{22}\text{N}_3\text{O}_7\text{S}$ $[\text{M}+\text{H}]^+$ 376.1173. Found: 376.1185.

3.4. Typical enzyme assay

Competitive inhibition of *H. pylori* AdT by compound **7a** (Fig. 5), with respect to Asp-tRNA^{Asn}, was characterized in 50 mM Hepes-KOH pH 7, 15 mM MgCl_2 , 25 mM KCl, 1 mM DTT, 2 mM ATP, and 1.28 mM L-glutamine, 0.50–2.00 μM Asp-tRNA^{Asn} and 6 nM AdT. V_0 is the uninhibited rate of product formation under these conditions, V_{max} the maximum rate, S the substrate concentration, V_i the inhibited rate and I the inhibitor concentration. According to Michaelis–Menten, in the absence of inhibitor, $V_0 = (V_{\text{max}}S)/(S + K_m)$, while in the presence of a competitive inhibitor, the reaction rate is $V_i = (V_{\text{max}}S)/(S + K_m(1 + I/K_i))$. Therefore, $V_i/V_0 = (S + K_m)/(S + K_m(1 + I/K_i))$. Curvefitting of the data to this equation was used to identify the competitive nature of this inhibition with respect to Asp-tRNA^{Asn}, and to calculate the K_i value. In all cases (except for compound **7e** which was poorly soluble) the K_i values obtained (Table 1) were within the range of the inhibitor concentrations

tested: chloramphenicol: 125–2000 μM ; **7a**: 5–1000 μM ; **7b**: 10–1660 μM ; **7c**: 100–1660 μM ; **7d**: 60–1000 μM ; **7e**: 60–1000 μM ; **7f**: 60–1000 μM .

Acknowledgments

This work was supported by the Natural Sciences and Engineering Research Council of Canada (NSERC) and the “Fonds de recherche sur la nature et les technologies, Québec (FQRNT)”. C.B. and J.H. thank NSERC and FQRNT for graduate scholarships, respectively.

References and notes

1. *The Aminoacyl-tRNA Synthetases*; Ibba, M., Francklyn, C., Cusack, S., Eds.; Eurekah.com/Landes Bioscience: Georgetown, TX, 2005.
2. *Translation Mechanisms*; Lapointe, J., Brakier-Gingras, L., Eds.; Landes Biosciences/Eurekah.com and Kluwer Academic/Plenum: New York, 2003.
3. Huot, J. L.; Lapointe, J.; Chênevert, R.; Bailly, M.; Kern, D. Glutamyl-tRNA and Asparaginyl-tRNA Biosynthetic Pathways. In Mander, L., Liu, H. W., Eds.; *Comprehensive Natural Products II Chemistry and Biology*; Elsevier: Oxford, 2010; Vol. 5, pp 383–431.
4. Feng, L.; Tumbula-Hansen, D.; Min, B.; Namgoog, S.; Salazar, J. C.; Orellana, O.; Söll, D. Transfer RNA-dependant Amidotransferases: Key Enzymes for Asn-tRNA and Gln-tRNA Synthesis in Nature. In *The Aminoacyl-tRNA Synthetases*; Ibba, M., Francklyn, C., Cusack, S., Eds.; Landes Biosciences: Georgetown, TX, 2005; pp 314–319.
5. Sheppard, K.; Sherrer, R. L.; Söll, D. *J. Mol. Biol.* **2008**, *377*, 845.
6. Schmitt, E.; Panvert, M.; Blanquet, S.; Mechulam, Y. *Structure* **2005**, *13*, 1421.
7. Nakamura, A.; Yao, M.; Chimnaronk, S.; Sakai, N.; Tanaka, I. *Science* **2006**, *312*, 1954.
8. Oshikane, H.; Sheppard, K.; Fukai, S.; Nakamura, Y.; Ishitani, R.; Numata, T.; Sherrer, R. L.; Feng, L.; Schmitt, E.; Panvert, M.; Blanquet, S.; Mechulam, Y.; Söll, D.; Nureki, O. *Science* **2006**, *312*, 1950.
9. Wu, J.; Bu, W.; Sheppard, K.; Kitabatake, M.; Kwon, S.-T.; Söll, D.; Smith, J. L. *J. Mol. Biol.* **2009**, *391*, 703.
10. Curnow, A. W.; Hong, K.-W.; Yuan, R.; Kim, S.-I.; Martins, O.; Winkler, W.; Henkin, T. M.; Söll, D. *Proc. Natl. Acad. Sci. U.S.A.* **1997**, *94*, 11819.
11. Ataide, S. F.; Ibba, M. *ACS Chem. Biol.* **2006**, *1*, 285.
12. Horiuchi, K. Y.; Harpel, M. R.; Shen, L.; Luo, Y.; Rogers, K. C.; Copeland, R. A. *Biochemistry* **2001**, *40*, 6450.
13. Decicco, C. P.; Nelson, D. J.; Luo, Y.; Shen, L.; Horiuchi, K. Y.; Amsler, K. M.; Foster, L. A.; Spitz, S. M.; Merrill, J. J.; Sizemore, C. F.; Rogers, K. C.; Copeland, R. A.; Harpel, M. R. *Bioorg. Med. Chem. Lett.* **2001**, *11*, 2561.
14. Huot, J. L.; Balg, C.; Jahn, D.; Moser, J.; Émond, A.; Blais, S. P.; Chênevert, R.; Lapointe, J. *Biochemistry* **2007**, *46*, 13190.
15. Balg, C.; Huot, J. L.; Lapointe, J.; Chênevert, R. *J. Am. Chem. Soc.* **2008**, *130*, 3264.
16. Schlünzen, F.; Zarivach, R.; Harms, J.; Bashan, A.; Tocilj, A.; Albrecht, R.; Yonath, A.; Franceschi, F. *Nature* **2001**, *413*, 814.
17. Moersch, G. W.; Hylander, D. P. *J. Am. Chem. Soc.* **1954**, *76*, 1703.
18. Marín-Martínez, F.; Sánchez-Meca, J. *Educ. Psychol. Meas.* **2010**, *70*, 56.
19. Drainas, D.; Mamos, P.; Coutsogeorgopoulos, C. *J. Med. Chem.* **1993**, *36*, 3542.
20. Vince, R.; Almquist, R. G.; Ritter, C. L.; Daluge, S. *Antimicrob. Agents Chemother.* **1975**, *8*, 439.
21. Michelinaki, M.; Mamos, P.; Coutsogeorgopoulos, C.; Kalpaxis, D. L. *Mol. Pharmacol.* **1997**, *51*, 139.
22. Hiratake, J. *Chem. Rec.* **2005**, *5*, 209.